Circadian and environmental signal transduction in a natural population of *Arabidopsis*

Dora L. Cano-Ramirez[1,2,7], Haruki Nishio[3,4,7], Tomoaki Muranaka[3,5], Luíza Lane de Barros Dantas[6], Mie N. Honjo[3], Jiro Sugisaka[3], Hiroshi Kudoh[3], Antony N. Dodd[6*].

1. Department of Plant Sciences, University of Cambridge, Downing Street, Cambridge, UK.

2. School of Biological Sciences, University of Bristol, Bristol, UK.

3. Center for Ecological Research, Kyoto University, Otsu, Shiga, Japan.

4. Data Science and AI Innovation Research Promotion Center, Shiga University, Hikone, Shiga, Japan.

5. Department of Environmental Sciences and Technology, Faculty of Agriculture, Kagoshima University, Korimoto, Kagoshima, Japan.

6. Department of Cell and Developmental Biology, John Innes Centre, Norwich, UK.

7. Equal contribution to this research.

* Corresponding author; antony.dodd@jic.ac.uk

Word counts: Main text (inc. methods) 5524; Abstract 198.

Abstract

Plants sense and respond to environmental cues during 24 h fluctuations in their environment. This requires the integration of internal cues such as circadian timing with environmental cues such as light and temperature to elicit cellular responses through signal transduction. The integration and transduction of circadian and environmental signals within plants growing in natural environments remain poorly understood. To gain insights into the 24 h dynamics of environmental signalling in nature, we performed a field study of cell signalling in a natural population of *Arabidopsis halleri.* As a representative model signalling pathway, we exploited the transduction of circadian and environmental signals from the nucleus to chloroplasts, by a sigma factor, to study diel cycles of environmental signalling under natural conditions. Using dynamic linear models to interpret the data, we identified that circadian regulation and temperature are key regulators of this pathway under natural conditions. We identified potential time-delay steps between pathway components, and diel fluctuations in the response of the pathway to temperature cues that are reminiscent of the process of circadian gating. This approach allowed us to identify dynamic integration and transduction of environmental cues, in the cells of plants, under naturally fluctuating diel cycles.

Introduction

Plants have sophisticated environmental sensing and signalling mechanisms that underpin their responses to the fluctuating environment. Under naturally fluctuating conditions, this requires signalling pathways that integrate dynamic, overlapping and complex environmental stimuli [1, 2]. These environmental fluctuations include the 24 h changes in environmental conditions that arise from the cycle of day and night. The 24 h environmental fluctuations have selected for the evolution of circadian clocks, which are endogenous biological oscillators that produce a cellular estimate of the time of day. Over each day, circadian rhythms structure the responses of plants to environmental fluctuations by aligning transcription, metabolism and development with the daily fluctuating environment [3-8]. In plants, environmental information including the light and temperature conditions is used to adjust the phase of the circadian oscillator, through the process of entrainment, so that the phase is aligned with the 24 h environmental cycle. This alignment between the circadian oscillator and the 24 fluctuating environment contributes to the fitness of plants [5].

Under natural conditions, circadian timing information is combined with environmental cues to establish a temporal program of gene expression [9]. For example, 97% of diel transcript profiles in field-grown rice can be predicted from meteorological data [9], and temperature cues regulate the alternative splicing of transcripts encoding circadian oscillator components in field-grown sugarcane [10]. Recent studies have provided insights into the diel organization of the transcriptome and metabolism, under field conditions, for several crops and natural plant populations [9-17]. However, the diel dynamics of environmental signalling pathways, with defined inputs and outputs, are less well understood under natural conditions. Understanding signal transduction in plants under natural conditions is a valuable part of translating laboratory studies into crop improvement. For example, this could contribute to forecasting the responses of ecosystems and crops to increasingly unpredictable climates [18]. Experiments conducted in controlled conditions that mimic components of field conditions remain unable to replicate all aspects of plant gene regulation

under natural conditions [17], so field experiments provide valuable insights into plant environmental responses.

To study the integration and transduction of circadian and environmental signals under naturally fluctuating conditions, we selected a well-characterized environmental signalling pathway as an experimental model. This comprises the regulation by the circadian clock of SIGMA FACTOR 5 (SIG5), which in turn regulates the transcription of *psbD* (Fig. 1A). *CCA1* and *SIG5* are nuclear encoded, and *psbD* is chloroplast encoded. We chose this pathway because it is relatively straightforward, consisting of three major components, each of which provides distinct regulatory points of signal transduction. Therefore, the pathway provides a relatively low level of complexity to evaluate circadian and environmental signal integration and transduction under realistic field conditions. CCA1 is a key component of the Arabidopsis circadian oscillator, and *CCA1* transcript abundance can be used as a proxy for the status of the circadian oscillator (Fig. 1A). SIG5 is a nuclear-encoded regulator of chloroplast transcription, which is regulated closely by the circadian oscillator under constant conditions [20]. Based on its responses under controlled conditions [19-30], we hypothesized that under natural conditions SIG5 might integrate information concerning circadian regulation, light quantity, light quality, temperature, and abiotic stress. Therefore, *SIG5* transcript abundance presents a read-out several environmental signal integration processes (Fig. 1A). It is thought that SIG5 is imported into chloroplasts, and communicates the integrated environmental information to chloroplast gene expression by regulating transcription from the blue light responsive promoter of *psbD* (*psbD* BLRP) [22] that encodes the D2 protein of Photosystem II (Fig. 1A). This chloroplast transcript provides an experimental read-out of a later step in this signalling pathway (Fig. 1A) [19, 20, 22].

We investigated the temporal dynamics of this signalling pathway in a natural habitat of the perennial *Arabidopsis* species, *Arabidopsis halleri* subsp. *gemmifera* (referred to here as *A. halleri*) [55]. The close-relatedness of *A. halleri* and *A. thaliana* makes it possible to identify pairs of homologous genes based on the sequence similarity (indicated by *Ahg* or *At* prefixes

to gene names) [56]. The circadian clock-SIG5-*psbD* BLRP pathway is present in *A. thaliana* and *A. halleri*, and well-conserved across the vascular plants [31, 32]. We obtained a number of time series, during two seasons of the year, that monitored pathway function under representative light and temperature conditions. We interpreted these data using dynamic linear models, which are a type of state space model derived from control theory. In these models, the state of the system can be predicted from the prior state of the system, onto which can be superimposed external effects. This allows the estimation of the dynamics of the system that arise from its internal dynamics and external factors (such as environmental cues). Using this approach, we identified key roles for temperature and the circadian clock in the regulation of this pathway under natural conditions, and obtained evidence for temporal gating of responses of the pathway to environmental cues. Our approaches could be applicable to the study of many circadian-regulated processes under naturally fluctuating conditions.

Results

Biological data underlying models of signal transduction

Under controlled conditions of constant light, *AtCCA1* and *AtSIG5* transcript abundance are very well correlated (Fig. S1A-D; data from [20]). This correlation between *AtCCA1* and *AtSIG5* transcript abundance is absent under light/dark cycles (Fig. S1E, F), suggesting that the integration of light and dark cues alters the diel regulation of *AtSIG5* transcript accumulation [19, 20]. We acquired time-series of transcript abundance during spring (March) and autumn/fall (September), close to the spring or autumn equinox (Fig. 1B-K; Fig. S2). Although both the spring and autumn equinoxes share 12-h photoperiods, they provide contrasting temperature regimes (cool and warm, respectively) (Fig. 1B, C; Fig. S2A, B), with irradiance levels determined by weather conditions (Fig. 1D, E; Fig. S2C, D). This allowed us to investigate temperature, light and seasonal influences upon SIG5-mediated signalling to chloroplasts, because the pathway is known to be affected by light and temperature in *A.*

thaliana [19, 21, 22, 26, 31]. We obtained data from areas with open sky and with vegetational shade, to include within our models the transcriptional responses to a wider range of irradiance levels (Fig. 1D, E; Fig. S3). The “sun” and “shade” sampling sites were chosen by measurement of the ratio of red to far-red light (R:FR) (Fig. S3C, D) and availability of plant patches, because *A. halleri* does not grow in deep shade at this location. The total light intensity at the sun sampling site was 5 to 10-fold greater during March 2015 than during September 2015, depending on the time of day, due to weather differences (Fig. 1D, E). During March 2015, the study site temperature at both sun and shade sites ranged from 0 °C to 17 °C (Fig. 1B, C). The temperature was often above 20 °C during September 2015, with greater diel fluctuations at the sun site (Fig. 1B, C).

We compared the pathway dynamics between the spring and autumn sampling periods by using a smooth trend model, and identified differences in pathway regulation (Fig. 1F-K and Fig. S2E-J). We estimated the parameters of a smooth trend model by Bayesian inference to visualize the differences in transcript abundance between the spring and autumn sampling. The morning peak accumulation of transcripts encoding the circadian clock component *AhgCCA1* was significantly greater during the autumn sampling compared with the spring, under both light conditions tested (Fig. 1F, G). During both sampling seasons, *AhgSIG5* transcripts reached peak abundance between the middle and end of the photoperiod (Fig. 1H, I). This differs from the phase of *AtSIG5* transcript accumulation under square-wave light/dark cycles under controlled conditions, where *AtSIG5* transcript abundance peaks around dawn [20]. The peak of the diel fluctuation of *AhgSIG5* was significantly greater during the March sampling period than during the September sampling period (Fig. 1H, I). Furthermore, the pre-dawn accumulation of *AhgSIG5* transcripts occurred at an earlier time during the dark period during September than during March (Fig. 1H, I). This delay in pre-dawn transcript accumulation might be due to weaker circadian control during the spring sampling period, as suggested by the significantly decreased peak height of *AhgCCA1* transcript oscillations during March compared with September (Fig. 1F, G). Transcripts

147 encoding the SIG5 regulatory target *AhgpsbD* BLRP (Fig. 1A) had a significantly greater
148 peak of accumulation during the September sampling season compared with the March
149 season, but only under the shade light conditions (Fig. 1J, K).

150 *AhgCCA1* transcript abundance was significantly greater under shade conditions during the
151 photoperiod, during both sampling seasons (Fig. S2E, F). This is reminiscent of the greater
152 *AtCCA1* promoter activity that occurs directly after dawn under controlled conditions of far
153 red light compared with red light [33]. We did not identify the diminished *AtCCA1* oscillation
154 that occurs under constant light with a very low R:FR [34] or on the shaded western side of
155 crop fields around dawn [16]. As with *AhgCCA1*, *AhgSIG5* transcript abundance was
156 significantly greater under shade than sun conditions, with this difference restricted to the
157 end of the photoperiod (Fig. S2G, H). *AhgpsbD* BLRP transcript levels were unaltered by the
158 two light environments (Fig. S2I, J).

159 **Time delays between signalling pathway components**

160 We assumed that SIG5-mediated signalling to chloroplasts involves a hierarchically-
161 organized pathway, whereby *AhgCCA1* is positioned upstream from the regulation of
162 *AhgSIG5* transcript accumulation, and *AhgpsbD* BLRP is positioned downstream of
163 AhgSIG5 activity (Fig. 1A). We also assumed that environmental signals might influence
164 *AhgCCA1*, *AhgSIG5* and *AhgpsbD* BLRP transcript accumulation independently (Fig. 1A)
165 [35]. To understand the dynamics of this process, we first considered the temporal
166 relationship between *AhgCCA1*, *AhgSIG5* and *AhgpsbD* BLRP transcript accumulation
167 under natural conditions (*t*1, *t*2; Fig. 1A). The abundance of each of these related transcripts
168 was monitored at each timepoint, but their responses to each other might not be
169 instantaneous. For example, in *A. thaliana* under controlled square-wave light/dark cycle
170 conditions, *AtCCA1* transcript abundance peaks at dawn, *AtSIG5* approximately 3 h after
171 dawn, and *AtpsbD* BLRP approximately 6 hours after dawn [20]. Comparable dynamics are
172 present in our field data, whereby *AhgCCA1* peaks at or after solar dawn (Fig. 1F, G),

173 *AhgSIG5* mid-photoperiod (Fig. 1H, I), and *AhgpsbD* BLRP towards the end of the
174 photoperiod under those conditions where it is rhythmic (Fig. 1J, K). Therefore, we reasoned
175 that there would be a time lag in the regulation of *AhgSIG5* by *AhgCCA1* (*t1* in Fig. 1A), and
176 in the regulation of *AhgpsbD* BLRP by *AhgSIG5* (*t2* in Fig. 1A).

177 We were interested to quantify these time lags, and use the information arising to construct
178 models that assess the regulation of the pathway by specific environmental variables. We
179 developed dynamic linear models that predict the abundance of *AhgSIG5* from *AhgCCA1*
180 transcript abundance, and predict *AhgpsbD* BLRP from *AhgSIG5* transcript abundance,
181 together with temperature and irradiance as explanatory variables. In these models, we used
182 the transcript abundance of the upstream component as an explanatory variable, and the
183 transcript abundance of the target component as a response variable within this analysis.
184 Therefore, *AhgSIG5* is the response variable in the first model with *AhgCCA1* as the
185 explanatory variable, whilst in the second model, *AhgSIG5* is used as the explanatory
186 variable for *AhgpsbD.* We tested the quality of model fit for a range of time delays (lags)
187 between the genes in the pathway (Fig. 1A). For this, we compared three model selection
188 parameters to estimate the time delay that provides the best estimation of the downstream
189 transcript (response variable). For a prediction of *AhgSIG5* from *AhgCCA1*, a model
190 containing a 6 h time lag produced the best model fit, according to three model selection
191 parameters (Fig. 2A, B, C). For a prediction of *AhgpsbD* BLRP from *AhgSIG5*, a model
192 containing a 4 h time lag produced the best model fit for two out of three model selection
193 parameters (Fig. 2D, E, F).

194 We detected differences between the two sampling seasons in the time lags that produced
195 the best model selection parameters (Fig. S4). During the March sampling season, the best
196 prediction of either *AhgSIG5* or *AhgpsbD* BLRP arose when time lags of 6-8 h (*AhgSIG5*
197 prediction from *AhgCCA1*) and 4-8 h (*AhgpsbD* BLRP prediction from *AhgSIG5*) were tested
198 (Fig. S4A-F). This was relatively longer than during the September sampling season, when
199 time lags of 0 or 4 h (*AhgSIG5* prediction from *AhgCCA1*) and 4 h (*AhgpsbD* BLRP

prediction from *AhgSIG5*) produced the best model fit estimates (Fig. S4G-L). This suggests that the low temperature in March delays the speed of signal transduction. Taken together, these analyses suggest that time delays in signalling pathways are detectable under field conditions, and that environmental conditions (seasonal differences in temperature, or seasonal regulation) might affect the speed of signal transduction.

Dynamics of environmental regulation of signalling pathway

Environmental fluctuations are complex, noisy, and occur in simultaneous combinations. This presents a challenge for interpreting time-series transcript data from the field within the context of environmental signalling. We elaborated upon our modelling approach to investigate the relationship between key environmental variables and SIG5-mediated signalling to chloroplasts under field conditions. We used statistical models, rather than models of biochemical kinetics [36], because this provides an effective tool for interpreting diel and seasonal transcriptome dynamics [9, 12, 37, 38]. Comparable approaches have allowed the investigation of diel and seasonal changes of transcriptome dynamics in *A. halleri* [12, 37, 38] and rice [9].

We represented the behaviour of the pathway components using dynamic linear models, into which the time delays that produced the best model fit were incorporated (Fig. 2). The output of the Bayesian estimation reproduced well the essential dynamics of the observed *AhgCCA1* transcript level (Fig. 3A, B). The model estimated a significant positive relationship between ambient temperature and *AhgCCA1* transcript abundance between midnight and midday, with no effect of temperature at other times (Fig. 3C). There was no significant effect of irradiance upon the estimation of *AhgCCA1* transcript abundance (Fig. 3D).

Diel fluctuations of *AhgSIG5* transcript abundance were reproduced well by the model (Fig. 3E, F). We identified a significant negative correlation between ambient temperature and *AhgSIG5* transcript level towards the end of the light period (Fig. 3G), whereas there was no

225 significant effect of irradiance upon the prediction of *AhgSIG5* transcript abundance (Fig.
226 3H). *AhgSIG5* is regulated by the circadian clock, and we included within the model
227 *AhgCCA1* transcript abundance as a proxy for circadian clock dynamics. There was a
228 significant positive coefficient of regression between *AhgCCA1* and *AhgSIG5* during the dark
229 period, and around the middle of the photoperiod (Fig. 3I).

230 Diel fluctuations of chloroplast *psbD* BLRP transcript abundance were also predicted well
231 (Fig. 3J, K). In this case, there was a significant positive coefficient of regression between
232 ambient temperature and *psbD* BLRP transcript abundance, which was restricted to the light
233 period (Fig. 3L). There was no significant coefficient of regression between irradiance and
234 *psbD* BLRP transcript abundance (Fig. 3M). *psbD* BLRP transcript accumulation is regulated
235 in *A. thaliana* by SIG5 [22], and within our model, there was a significant positive coefficient
236 of regression between *AhgSIG5* and *AhgpsbD* BLRP transcript levels during part of the light
237 period (Fig. 3N).

238 Together, this analysis identifies that the ambient temperature, rather than the irradiance,
239 was important for predicting the dynamics of all pathway components under naturally
240 fluctuating conditions. In addition, the effect of the circadian clock (*AhgCCA1*) contributed to
241 the prediction of *AhgSIG5* transcript abundance (Fig. 3I), and the effect of SIG5 contributed
242 to the prediction of *AhgpsbD* BLRP transcript abundance (Fig. 3N). A feature within these
243 predictions was the restriction to specific times of day of significant coefficients of regression
244 between transcripts abundance and certain variables (such as for temperature in the
245 prediction of *AhgCCA1* (Fig. 3C) and *AhgSIG5* (Fig. 3G)). These 24-h fluctuations in the
246 coefficient of regression are suggestive of the concept of circadian gating, which is the
247 process whereby the circadian clock constrains certain biological processes to specific times
248 in the 24 h cycle [39]. In plants, this often takes the form of a circadian rhythm in the
249 magnitude of the response to identical environmental stimuli given at different times of day
250 [8].

Temporal gating of temperature regulation of SIG5-mediated signalling to chloroplasts under natural conditions

Our dynamic linear modelling analysis suggested that under natural conditions, greater ambient temperatures upregulate *AhgCCA1* and *AhgpsbD* BLRP transcript levels, whereas lower ambient temperatures upregulate *AhgSIG5* transcript levels (Fig. 3C, G, L). We tested this hypothesis by applying moderate temperature manipulations to adjacent patches of *A. halleri* plants, in the field, using custom-designed equipment (Fig. 4A; Fig. S5). We collected 24-h time-series of RNA samples from these plant patches, and interpreted the data with smooth trend models. The moderate temperature increase caused a small significant upregulation of *AhgCCA1* transcript abundance after dawn relative to the control, whereas the temperature reduction treatment was without effect (Fig. 4B). The moderate temperature increase was without effect upon *AhgSIG5* transcript abundance, whereas the temperature reduction treatment upregulated *AhgSIG5* transcripts significantly immediately after dawn, relative to the control, and caused a significant reduction in transcript abundance during the afternoon (Fig. 4C). This is consistent with the negative coefficient of regression between *AhgSIG5* and temperature under naturally fluctuating conditions (Fig. 3G), and with the upregulation of *A. thaliana SIG5* by a short cold treatment under laboratory conditions [22]. The restriction of the response of *AhgSIG5* transcripts to the moderate temperature reduction (Fig. 4C) is consistent with the 24-h cycle of the magnitude of the coefficient of regression of temperature for *AhgSIG5* transcript abundance (Fig. 3G). This further supports the notion of temporal gating of the influence of temperature upon this pathway under naturally fluctuating conditions.

Transcripts for the chloroplast target of SIG5, *AhgpsbD* BLRP, were also altered by temperature manipulation. The moderate temperature elevation significantly increased *AhgpsbD* BLRP transcript levels relative to the control, whereas the moderate temperature reduction significantly reduced *AhgpsbD* BLRP transcripts relative to the control. These significant alterations were restricted to the photoperiod, which might be because chloroplast

278 DNA binding and transcription by PEP generally requires light [40-44]. Furthermore, the
279 positive regulation of *AhgpsbD* BLRP transcript abundance by the temperature
280 manipulations (Fig. 4D) is consistent with the coefficient of regression between *AhgpsbD*
281 BLRP transcript abundance and temperature under naturally fluctuating conditions (Fig. 3L).

282 **Discussion**

283 We established that circadian regulation and ambient temperature are potential regulators of
284 *AhgSIG5*-mediated signalling to chloroplasts, in a natural population of *A. halleri*. Our
285 analysis identified a significant regulation of *AhgSIG5* by *AhgCCA1* from midnight to morning
286 (Fig. 3I), and significant regulation of *AhgpsbD* BLRP by *AhgSIG5* towards the end of the
287 photoperiod (Fig. 3N). These significant relationships suggest that under natural conditions,
288 a signal is communicated from the circadian oscillator (using *AhgCCA1* as a proxy) to the
289 signalling pathway output of *AhgpsbD* BLRP. One interpretation is that the pathway couples
290 the circadian oscillator and temperature response processes to chloroplast gene
291 transcription under naturally fluctuating conditions.

292 We identified seasonal differences in the maximum accumulation of *AhgCCA1*, *AhgSIG5*
293 and *AhgpsbD* BLRP. *AhgCCA1* and *AhgpsbD* BLRP had significantly lower peak
294 accumulation during the spring sampling period compared with the autumn sampling
295 season. In comparison, *AhgSIG5* had significantly greater peak accumulation during the
296 spring compared with the autumn sampling season. The difference in *AhgCCA1* dynamics
297 between these sampling seasons likely reflects the decreased amplitude of the circadian
298 oscillator that occurs under lower temperature conditions, in both controlled environments
299 and the field [12, 45-47]. The difference in dynamics of *AhgSIG5* compared with *AhgCCA1*
300 suggests that an additional temperature input into this pathway occurs between the circadian
301 oscillator and *AhgSIG5*. In *A. thaliana*, *SIG5* transcripts are upregulated by short cold
302 temperature treatments [22] and in our field experiment, *AhgSIG5* transcript accumulation
303 had a negative coefficient of regression with the temperature (Fig. 3G, Fig. 4C). This

304 negative coefficient of regression predicts that under lower temperature conditions, *AhgSIG5*
305 transcript abundance will increase. Therefore, the lower temperatures of the spring sampling
306 season compared with the autumn sampling season (Fig. 1A, B) might explain the greater
307 levels of *AhgSIG5* transcript accumulation during the spring.

308 Because we considered *AhgpsbD* BLRP to represent the ultimate output from the signalling
309 pathway (Fig. 1A), our analysis suggests that environmental inputs occurred within at least
310 three positions in the pathway; first, in the regulation of *AhgCCA1* transcript accumulation by
311 the season or temperature, second, in the regulation of *AhgSIG5* transcript accumulation by
312 temperature, and, a third environmental input occurring downstream of *AhgSIG5* transcript
313 accumulation for the regulation of *AhgpsbD* BLRP. This is evidenced by the differences in
314 temperature responses of *AhgCCA1* (positive relationship), *AhgSIG5* (negative relationship),
315 and *AhgpsbD* BLRP (positive relationship) (Fig. 3C, G, L). These environmental inputs might
316 occur through biologically independent processes, such as temperature inputs to the
317 circadian clock mediated by temperature-responsive components such as the evening
318 complex [48, 49]. One of these mechanisms could be the regulation of *AhgSIG5* by HY5,
319 which is a known regulator of SIG5 that participates in low-temperature gene regulation [22,
320 25, 50] and binds the SIG5 promoter in *A. thaliana* [51]. Furthermore, there might be direct
321 effects of light upon sigma factor activity in chloroplasts through, for example, redox
322 regulation [52] or light- and temperature-regulation of chloroplast protein import. We did not
323 consider here the long history of light or temperature conditions upon leaves prior to
324 experimentation [53], or other biotic or abiotic factors such as water availability, relative
325 humidity, and atmospheric CO_2 concentration.

326 Statistical modelling of the transcriptome of field-grown *Oryza sativa* (rice) concluded that
327 the main environmental driver of *OsSIG5* (*Os05g0586600*) transcript accumulation is
328 temperature [9]. In this case, the temperature had a negative regression coefficient with
329 *OsSIG5* [9]. This is consistent with our finding of a negative coefficient of regression
330 between temperature and *AhgSIG5*. The study of the rice transcriptome in the field [9] did

not monitor chloroplast-encoded transcripts, so a direct comparison between *AhgpsbD* BLRP and our data is not possible.

A key finding from our work is the detection of a 24 h fluctuation in the coefficient of regression between the three genes and temperature (Fig. 3C, G, L). One interpretation of this is that there is a diel cycle of sensitivity of these pathway components to temperature cues, with their response to temperature restricted to certain times of day. This is reminiscent of circadian gating, which is the phenomenon whereby the circadian oscillator restricts the response to a stimulus to certain times of day [39]. These findings are corroborated by laboratory experiments, which demonstrate that the circadian oscillator gates its own response to temperature [54], and the response of *AhgSIG5* to blue light is gated by the circadian oscillator [20]. This is important, because it suggests that processes of circadian gating might operate under naturally fluctuating conditions to modulate the environmental responses of plants.

Our investigation provides insights into molecular aspects of signal transduction in plants under field conditions. This represents a relatively under-studied topic, and we developed new quantitative approaches to interpret transcript data collected under complex fluctuating environments, to investigate a specific pathway. This allowed us to identify potential time-delay steps within a signalling mechanism, multiple positions of environmental inputs, and temporal gating of a response to temperature. The approaches used provide a framework to study environmental signal integration in plants and other organisms under field conditions, which might be valuable to understanding rhythmic biological responses within an increasingly unpredictable climate.

Materials and Methods

Field site and plant material

Our experiments used a naturally-occurring population of *Arabidopsis halleri* subsp. *gemmifera* (Matsum.) growing beside a forested stream in Hyogo Prefecture, Japan (Omoide-gawa site; 35°06' N, 134°55' E, elevation 190–230 m) [12, 37, 55] (Fig. 1B, C). We selected *A. halleri* as an experimental model for several reasons [56]. First, it has a high nucleotide sequence identity and good synteny with *A. thaliana* [57]. Second, unlike *A. thaliana*, the perennial life history of *A. halleri* allows investigation of transcriptional responses across the seasons [2, 55]. Many individuals are clones because the species propagates by producing clonal rosettes as well as by seeds, which allows repeated sampling from single genotypes. Furthermore, *A. halleri* is metal tolerant and occurs in natural habitats that are relatively free from other vegetation due to contamination by heavy metals, which provides experimentally-convenient sites enriched with many *A. halleri* plants [58]. *Arabidopsis halleri* subsp. *gemmifera* at this site was previously identified by examination of museum and herbarium specimens, and a nearby population provided material for sequencing the *A. halleri* genome [55, 57]. Sampling occurred during 24 – 26 March 2015, 15 – 17 September 2015, and 13 - 14 September 2016, where March and September correspond to spring and autumn (fall) at the field site, respectively.

The *A. halleri* homologs of the *A. thaliana* genes *CCA1* and *SIG5* are loci *g25274* (*AhgSIG5*) and *g097040* (*AhgCCA1*), respectively. These were identified from *A. halleri* genome Version Ahal2.2 [57]. *AhgSIG5* has 94.9% coding sequence identity and 95.0% protein sequence identity with the *A. thaliana* homolog. *AhgCCA1* has 94.8% coding sequence identity and 93.3% protein sequence identity with the *A. thaliana* homolog. Chloroplast-encoded *psbDC* is not annotated within Version Ahal2.2 of the *A. halleri* genome, and we identified this instead within scaffold 2 of an *A. halleri* reference transcriptome [59]. The

AhgpsbD BLRP promoter region, which was our focus, has a 100% sequence identity with *psbD* BLRP of *A. thaliana* [41].

Sampling under natural and manipulated conditions

The first sets of samples were obtained under natural conditions without environmental manipulation. For this, we sampled during two different seasons, March 2015 and September 2015, on dates that were close to the spring and autumn equinox. We exploited variations in environmental conditions across the field site, and sampled leaves from the locations nominated as “sun” and “shade” sites. At “sun” locations, plants received direct sunlight during the day, and at “shade” locations plants received sunlight filtered by surrounding vegetation for most of the day with the sites identified by measurement of the ratio of red to far red light (Fig. S3; R:FR calculated as the photon irradiance from 660 to 670nm divided by the photon irradiance from 725 to 735nm [60]). In each case, sampling occurred for at least 24 h. During March 2015, plants received more direct sunlight, whereas during September 2015 the light was scattered through sky overcast with clouds.

We expanded the range of environmental conditions by manipulating the temperature conditions around patches of plants (September 2016). In addition to control plants that were not manipulated (Fig. S5A), we applied two temperature treatments. These were (1) a continuous temperature increase (Fig. S5B), whereby plants were covered with clear plastic horticultural domes to block air currents and trap warm air; (2) a continuous temperature reduction, using a custom device that passed air through a duct within a heat-exchanging ice-filled polystyrene box and expelled the chilled air into a clear horticultural dome covering the plants, with chilling augmented by small ice packs within the dome (Fig. S5C).

Field sampling for transcript analysis

Across all experimental conditions, the same sampling and RNA isolation procedures were used. At 2 h intervals, a fully expanded rosette leaf was excised with dissecting scissors

from 6 replicate plants for each condition. The time-courses using naturally occurring sun and shade conditions each comprised 13 sampling timepoints over a total of 26 hours, and the time-courses involving artificial temperature manipulations comprised 15 sampling timepoints over a total of 30 hours. Sampled leaves were placed immediately into individual microtubes containing at least 400 µL RNALater (Invitrogen). Scissors and forceps were cleaned with 70% (w/v) ethanol between samples. After sampling, tubes were placed temporarily on dry ice for up to 2 hours, at -40 °C for 3 days in a portable freezer during transfer to the laboratory, and then at -80 °C until RNA isolation. During hours of darkness, sampling occurred using green-filtered head torches. Each sampling timepoint was from the same set of replicate plants. We obtained a separate reference standard for all RT-qPCR experiments in the study, by pooling RNA from 10 leaves sampled at midday during March 2015 from healthy plants located randomly across the study site. This provided a reference cDNA sample against which all RT-qPCR analyses from all sampling seasons were normalized, to allow comparability between all datasets. This reference RNA sample was collected during March 2015. In all experiments, dawn and dusk were defined as the astronomical (solar) time of sunrise and sunset.

RNA isolation and RT-qPCR

Frozen samples containing RNALater were defrosted in a cold room for 4 hours, the RNALater was removed, and leaf tissue was transferred to new dry tubes and frozen in liquid nitrogen. Frozen tissue was ground with a TissueLyzer and total RNA was isolated from the powdered plant material using Macherey-Nagel Nucleospin II RNA extraction kits (Thermo-Fisher). cDNA was synthesized using a High Capacity cDNA Reverse Transcription Kit (Applied Biosystems) supplemented with RNAase inhibitor, as described previously [19, 20]. RNA concentrations were determined using a Nanodrop spectrophotometer (Thermo Scientific). cDNA was synthesized using an ABI High Capacity cDNA Reverse Transcription Kit (Applied Biosystems) according to the manufacturer's instructions, using random primers for the cDNA synthesis reaction. 1:500 cDNA dilutions were analysed using Brilliant III Ultra-

Fast SYBR Green QPCR master mix (Agilent Technologies) and required primer pairs (Table S2). Primers were designed using the PrimerQuest™ Tool from Integrated DNA Technologies. Results were normalized using the ΔΔCt method to *AhgACTIN2* [19, 20]. *AhgACTIN2* is encoded in *A. halleri* by locus *g21632* [57] and has 97.8% coding sequence identity with *A. thaliana ACTIN2* (*At3g18780*). Statistical comparisons within transcript abundance data were conducted using the SPSS software package.

Environmental monitoring

The temperature and irradiance were measured beside the plants during sampling. The temperature at each location, for each environmental manipulation, was monitored with EL-USB-2 data loggers (Lascar Electronics) at 5-minute intervals. Temperature loggers were wrapped in aluminium foil to prevent surface heating by solar radiation. Irradiance was measured using a CC-3-UV-S cosine corrector connected to a USB2000+ spectrometer with a QP400-2-UV-VIS fibre optic cable (Ocean Optics). Ambient light spectra (200 nm to 900 nm) were collected every 5 minutes over the 14 hours of light during each day of sampling using OceanView software (Ocean Optics) on a laptop PC, controlled by a custom script. The spectrometer and computer were powered using portable lithium battery packs (Powertraveller, Hampshire, UK).

Smooth trend model analysis

The smooth trend model (STM) to analyze the difference in transcript abundance between March and September under sun and shade conditions (Fig. 1) was defined by the equations:

$$\mu_{1,t} \sim Normal(2\mu_{1,t-1} - \mu_{1,t-2},\ \sigma_{\mu 1}^2), \quad (1)$$

$$\delta_t \sim Cauchy(\delta_{t-1},\ \sigma_{\delta}^2), \quad (2)$$

$$\mu_{2,t} = \mu_{1,t} + \delta_t, \quad (3)$$

$$y_{1,t} \sim Normal(\mu_{1,t},\ \sigma_y^2), \quad (4)$$

$$y_{2,t} \sim Normal(\mu_{2,t},\ \sigma_y^2), \quad (5)$$

where μ_1 and μ_2 are the smooth trend components in March and September in 2015, respectively, δ_t is the time-varying difference between the two seasons, and y_1 and y_2 are the observed transcript abundance in the two seasons. $t = (1, 2, \cdots, 13)$ is the time point at two-hour intervals. The same STM was used to analyze the difference in transcript abundance between sun and shade conditions in March and September (Fig. S1).

The parameters of the models were estimated by Bayesian inference. The statistical models were written in the Stan language and the programs were called by the rstan package (using version 2.21.0 of R). After 2,000 warm-up steps, 1,000 Markov Chain Monte Carlo (MCMC) samples were obtained by thinning out 6,000 MCMC samples for each of four parallel chains. Thus, 4,000 MCMC samples were obtained in total.

For the models of the three (ambient, warm and chill) conditions in the local environment manipulation experiment, additional δ, μ and y were considered:

$$\delta_{2,t} \sim Cauchy(\delta_{2,t-1},\ \sigma_{\delta 2}^2), \quad (6)$$

$$\mu_{3,t} = \mu_{1,t} + \delta_{2,t}, \quad (7)$$

$$y_{3,t} \sim Normal\left(\mu_{3,t},\ \sigma_y^2\right). \quad (8)$$

Dynamic linear model

The dynamic linear model (DLM) to analyze the time-varying effect of environmental variables on transcript abundance (Fig. 2) was defined by the equations:

$$\mu_t \sim Normal(\mu_{t-1},\ \sigma_\mu^2), \tag{9}$$

$$\beta_{temp,t} \sim Normal(\beta_{temp,t-1},\ \sigma_{\beta temp}^2), \tag{10}$$

$$\beta_{light,t} \sim Normal(\beta_{light,t-1},\ \sigma_{\beta light}^2), \tag{11}$$

$$\alpha_{MarSun,t} = \mu_t + \beta_{temp,t} \cdot temp_{MarSun,t} + \beta_{light,t} \cdot light_{MarSun,t}, \tag{12}$$

$$\alpha_{MarShade,t} = \mu_t + \beta_{temp,t} \cdot temp_{MarShade,t} + \beta_{light,t} \cdot light_{MarShade,t}, \tag{13}$$

$$\alpha_{SepSun,t} = \mu_t + \beta_{temp,t} \cdot temp_{SepSun,t} + \beta_{light,t} \cdot light_{SepSun,t}, \tag{14}$$

$$\alpha_{SepShade,t} = \mu_t + \beta_{temp,t} \cdot temp_{SepShade,t} + \beta_{light,t} \cdot light_{SepShade,t}, \tag{15}$$

$$y_{MarSun,t} \sim Normal(\alpha_{MarSun,t},\ \sigma_y^2), \tag{16}$$

$$y_{MarShade,t} \sim Normal(\alpha_{MarShade,t},\ \sigma_y^2), \tag{17}$$

$$y_{SepSun,t} \sim Normal(\alpha_{SepSun,t},\ \sigma_y^2), \tag{18}$$

$$y_{SepShade,t} \sim Normal(\alpha_{SepShade,t},\ \sigma_y^2), \tag{19}$$

where μ is the trend component, β is the time-varying regression coefficient, α is the true state of transcript abundance, y is the observed transcript abundance, and σ^2 is the variance. The subscripts, $temp$, $light$, Mar, Sep, Sun and $Shade$ represent temperature, irradiance, March, September, sun condition and shade condition, respectively. $t = (1, 2, \cdots, 13)$ is the time point at two-hour intervals.

In the *AhgSIG5* and *AhgpsbD* BLRP models, the effects of the upstream genes (i.e., *AhgCCA1* in the *AhgSIG5* model and *AhgSIG5* in the *AhgpsbD* BLRP model) were additionally considered. Thus, the equations of α are modified as follows:

$$\alpha_{MarSun,t} = \mu_t + \beta_{temp,t} \cdot temp_{MarSun,t} + \beta_{light,t} \cdot light_{MarSun,t} + \beta_{gene,t} \cdot gene_{MarSun,t}, \quad (20)$$

$$\alpha_{MarShade,t} = \mu_t + \beta_{temp,t} \cdot temp_{MarShade,t} + \beta_{light,t} \cdot light_{MarShade,t} + \beta_{gene,t} \cdot gene_{MarShade,t}, \quad (21)$$

$$\alpha_{SepSun,t} = \mu_t + \beta_{temp,t} \cdot temp_{SepSun,t} + \beta_{light,t} \cdot light_{SepSun,t} + \beta_{gene,t} \cdot gene_{SepSun,t}, \quad (22)$$

$$\alpha_{SepShade,t} = \mu_t + \beta_{temp,t} \cdot temp_{SepShade,t} + \beta_{light,t} \cdot light_{SepShade,t} + \beta_{gene,t} \cdot gene_{SepShade,t}, \quad (23)$$

where $gene$ is the mean transcript abundance of the upstream genes, and the other symbols are the same as above. The lagged effects of the upstream genes were tested by using values at previous time points (e.g., using $gene_{MarSun,t-1}$, $gene_{MarSun,t-2}$, $gene_{MarSun,t-3}$ or $gene_{MarSun,t-4}$ for $\alpha_{MarSun,t}$). The same DLM was used in Fig. 2 and S4.

The parameters of the models were estimated by Bayesian inference. The statistical models were written in the Stan language and the programs were compiled using CmdStan (version 2.24). To operate CmdStan, the cmdstanr package (version 0.4.0) of R was used. After 3,000 warm-up steps, 1,000 MCMC samples were obtained for each of the four parallel chains, and thus 4,000 MCMC samples were obtained in total.

Acknowledgements

We thank Noriane M. L. Simon and Tasuku Ito for experimental assistance, and Paige E. Panter and Deirdre A. Lynch for constructive feedback. This research was funded by BBSRC (UK) (BB/I005811/2; BB/J014400/1; Institute Strategic Programme GEN BB/P013511/1), The Royal Society (IE140501), The Leverhulme Trust (RPG-2018-216), the

Japan Society for Promotion of Science (JSPS KAKENHI, JP21H04977, JP21H05659, JP21K15164), the Japan Science and Technology Agency (JST, CREST no. JPMJCR1501) and the Bristol Centre for Agricultural Innovation. DLCR is grateful to Consejo Nacional de Ciencia y Tecnología (Mexico) for awarding a scholarship. This research was conducted through the Joint Usage programme of the Center for Ecological Research of Kyoto University.

Author contributions

DLCR, HN, JS, MNH, HK and AND designed and performed experimentation; HN, DLCR, TM, LLBD, HK and AND analysed and interpreted data, and DLCR, HN, LLBD, HK and AND wrote the paper.

Competing interests

The authors declare no competing interests

Figure legends

Fig. 1. Components of a circadian signalling pathway have diel fluctuations in a natural plant population. (A) Potential architecture of a signal transduction pathway underlying SIG5-mediated signalling to chloroplasts, with environmental inputs occurring at several positions. *t1* and *t2* represent the time taken for signal transduction between each pathway component. (B-E) Diel fluctuations in (B, C) ambient temperature and (D, E) total irradiance detected (200-900 nm), measured at 5-minute intervals. (F-K) Bayesian estimation of smooth trend model (STM) for March and September 2015. The output of STM for (F, G) *AhgCCA1*, (H, I) *AhgSIG5* and (J, K) *AhgpsbD BLRP*. In F-K, the upper graphs show the predicted relative transcript abundance for March (pink) and September (brown) with the mean of observed values (dots), and the lower graphs represent the differences in transcript abundance between March and September. The solid line and the shaded region are the median and

513 the 95% credible interval of the posterior distribution. When the 95% credible interval of the
514 difference between March and September does not contain zero, the difference is
515 considered significant.

516 **Fig. 2.** Time-delay steps are predicted within this signalling pathway under naturally-
517 fluctuating conditions. Lagged effects of variables in Bayesian estimation of dynamic linear
518 models (DLM) for transcript levels during March and September 2015. (A, B, C) RMSE, log-
519 likelihood and correlation of the models to predict *AhgSIG5* against the observed values,
520 incorporating time lags of the upstream *AhgCCA1*. (D, E, F) RMSE, log-likelihood and
521 correlation of the models to predict *AhgpsbD BLRP* against the observed values,
522 incorporating time lags of the upstream *AhgSIG5*. The time lags of temperature and
523 irradiance are set to 0. Asterisks represent (A, D) the lowest RMSE, (B, E) the highest log-
524 likelihood and (C, F) the highest correlation. Error bars represent the 95% Bayesian credible
525 intervals.

526 **Fig. 3.** The circadian clock and ambient temperature are key regulators of SIG5-mediated
527 signalling to chloroplasts under naturally-fluctuating conditions. Bayesian estimation of the
528 dynamic linear model (DLM) for March and September 2015. (A-D) The output of DLM for
529 *AhgCCA1* where relative transcript abundance for (A) sun condition and (B) shade condition,
530 with the coefficient of regression for (C) temperature and (D) irradiance. (E-I) The output of
531 DLM for *AhgSIG5*, where (I) the coefficient of regression for *AhgCCA1* is shown, with other
532 plots the same as (A-D). (J-N) The output of DLM for *AhgpsbD BLRP*, where (N) is the
533 coefficient of regression for *AhgSIG5* is shown, with other plots the same as (A-D). The
534 predicted relative transcript abundance for March (orange) and September (blue) are shown
535 with the mean of observed values (dots). In each graph, the solid line and the shaded region
536 are the median and the 95% credible interval of the posterior distribution.

537 **Fig. 4.** Prediction of diel rhythms of gating of temperature response in a natural plant
538 population. Bayesian estimation of smooth trend model (STM) for temperature manipulation

539 experiments in September 2016. (A) Temperature changes during the study period in each
540 condition. (B-D) The output of STM for (B) *AhgCCA1*, (C) *AhgSIG5* and (D) *AhgpsbD BLRP*.
541 In each panel, the upper graphs show the predicted relative transcript abundance for
542 ambient (black), warm (red) and cool (light blue) conditions with the mean of observed
543 values (dots), and the lower graphs represent the differences in transcript abundance
544 against the ambient condition. In each graph, the solid line and the shaded region are the
545 median and the 95% credible interval of the posterior distribution. When the 95% credible
546 interval of the difference between conditions does not contain zero, the difference is
547 considered significant.

548 **Fig. S1.** Close relationship between *AtCCA1* and *AtSIG5* transcript abundance under free-
549 running conditions in *A. thaliana* under controlled conditions. (A-D) Relationship between
550 *AtCCA1* and *AtSIG5* transcript abundance under conditions of constant light, from the
551 transcriptome studies of (A) [3] (B) [53], (C) [4], (D) [6]. (E, F) Relationship between *AtCCA1*
552 and *AtSIG5* transcript abundance under light/dark cycles with (E) long and (F) short
553 photoperiods, from the transcriptome study of [54]. Blue lines indicate a regression line.
554 Pearson's correlation coefficient (R) with p-values testing for the likelihood of a chance
555 correlation are shown for each plot.

556 **Fig. S2.** Components of a circadian signalling pathway have diel fluctuations in a natural
557 plant population. Bayesian estimation of smooth trend model (STM) comparing sun and
558 shade conditions, sampled during 2015. (A-D) Diel fluctuations in total irradiance detected
559 (A, B; 200-900 nm) and (C, D) ambient temperature, measured at 5-minute intervals. (E-J)
560 The output of STM for (E, F) *AhgCCA1*, (G, H) *AhgSIG5* and (I, J) *AhgpsbD* BLRP. In E-J,
561 the upper graphs show the predicted relative transcript abundance for sun (orange) and
562 shade (light grey) conditions, with the mean of observed values (dots). The lower graphs
563 represent the differences in transcript abundance between sun and shade conditions. The
564 solid line and the shaded region are the median and the 95% credible interval of the

posterior distribution. When the 95% credible interval of the difference between sun and shade conditions does not contain zero, the difference is considered significant.

Fig. S3. Effects of the ratio of red to far-red light upon *A. halleri* plants in the field, during March and September sampling seasons. (A, B) Examples of rosette-stage plants growing under (A) sun and (B) shade conditions during the September sampling season. (C, D) Comparison of the ratio of red to far-red light received by plants under the sun- and shade conditions during (C) March 2015 and (D) September 2015 sampling seasons. The R:FR varied during the photoperiod during both sampling seasons, and the effect of shade on R:FR was ameliorated by heavy cloud cover.

Fig. S4. The nature of the time-delay steps within this signalling pathway depends on the sampling season. Lagged effects of variables in Bayesian estimation of the dynamic linear model (DLM) for March and September separately in 2015. (A, D, G, J) RMSE, (B, E, H, K) log-likelihood and (C, F, I, L) correlation of the models to predict *AhgSIG5* in March against the observed values, incorporating time lags of *AhgCCA1*. (D-F) RMSE, log-likelihood and correlation of the models to predict *AhgpsbD* BLRP in March against the observed values, incorporating time lags of *AhgSIG5*. (G-I) RMSE, log-likelihood and correlation of the models to predict *AhgSIG5* in September against the observed values, incorporating time lags of *AhgCCA1*. (J-L) RMSE, log-likelihood and correlation of the models to predict *AhgpsbD* BLRP in September against the observed values, incorporating time lags of *AhgSIG5*. Time lags of temperature and irradiance are set to 0. Asterisks represent the lowest RMSE (A, D, G, J), the highest log-likelihood (B, E, H, K) and the highest correlation (C, F, I, L). Error bars represent the 95% Bayesian credible intervals.

Fig. S5. Moderate temperature manipulations to adjacent patches of *A. halleri* plants, in the field, using custom-designed equipment. (A) The representative appearance of plant patches under naturally fluctuating conditions. (B) Plants covered with a plastic dome to raise temperature. (C) Plants covered with plastic dome undergoing temperature reduction with a

591 custom chilling device. In this device, cool air is introduced to enclosed plant patches after
592 being driven slowly through a heat exchanger, positioned within an expanded polystyrene
593 box filled with ice.

594 **Fig. S6.** Location of field sampling. Photographs of (A) upstream and (B) downstream views
595 of Omoide river site, which has naturally occurring populations of *A. halleri*. The majority of
596 plants at ground level on the stony river banks are *A. halleri*.

597 **References**

598 1. Millar, A.J., *The intracellular dynamics of circadian clocks reach for the light of*
599 *ecology and evolution.* Annual Review of Plant Biology, 2016. **67**(1): p. 595-618.
600 2. Kudoh, H., *Molecular phenology in plants: in natura systems biology for the*
601 *comprehensive understanding of seasonal responses under natural environments.*
602 New Phytologist, 2016. **210**(2): p. 399-412.
603 3. Covington, M.F., et al., *Global transcriptome analysis reveals circadian regulation of*
604 *key pathways in plant growth and development.* Genome Biology, 2008. **9**(8): p.
605 R130.
606 4. Edwards, K.D., et al., *FLOWERING LOCUS C mediates natural variation in the high-*
607 *temperature response of the Arabidopsis circadian clock.* The Plant Cell, 2006. **18**(3):
608 p. 639-650.
609 5. Dodd, A.N., et al., *Plant circadian clocks increase photosynthesis, growth, survival,*
610 *and competitive advantage.* Science, 2005. **309**(5734): p. 630-633.
611 6. Harmer, S.L., et al., *Orchestrated transcription of key pathways in Arabidopsis by the*
612 *circadian clock.* Science, 2000. **290**(5499): p. 2110-2113.
613 7. Graf, A., et al., *Circadian control of carbohydrate availability for growth in Arabidopsis*
614 *plants at night.* Proceedings of the National Academy of Sciences, 2010. **107**(20): p.
615 9458-9463.
616 8. Hotta, C.T., et al., *Modulation of environmental responses of plants by circadian*
617 *clocks.* Plant, Cell & Environment, 2007. **30**(3): p. 333-349.
618 9. Nagano, Atsushi J., et al., *Deciphering and prediction of transcriptome dynamics*
619 *under fluctuating field conditions.* Cell, 2012. **151**(6): p. 1358-1369.
620 10. Dantas, L.L.B., et al., *Alternative splicing of circadian clock genes correlates with*
621 *temperature in field-grown sugarcane.* Frontiers in Plant Science, 2019. **10**: p. article
622 1614.
623 11. Dantas, L.L.B., et al., *Rhythms of transcription in field-grown sugarcane are highly*
624 *organ specific.* Scientific Reports, 2020. **10**(1): p. article 6565.
625 12. Nagano, A.J., et al., *Annual transcriptome dynamics in natural environments reveals*
626 *plant seasonal adaptation.* Nature Plants, 2019. **5**(1): p. 74-83.
627 13. Matsuzaki, J., Y. Kawahara, and T. Izawa, *Punctual transcriptional regulation by the*
628 *rice circadian clock under fluctuating field conditions.* The Plant Cell, 2015. **27**(3): p.
629 633-648.
630 14. Annunziata, M.G., et al., *Response of Arabidopsis primary metabolism and circadian*
631 *clock to low night temperature in a natural light environment.* Journal of Experimental
632 Botany, 2018. **69**(20): p. 4881-4895.

15. Annunziata, M.G., et al., *Getting back to nature: a reality check for experiments in controlled environments.* Journal of Experimental Botany, 2017. **68**(16): p. 4463-4477.
16. Dantas, L.L.B., et al., *Field microenvironments regulate crop diel transcript and metabolite rhythms.* New Phytologist, 2021. **232**(4): p. 1738-1749.
17. Hashida, Y., et al., *Fillable and unfillable gaps in plant transcriptome under field and controlled environments.* Plant, Cell & Environment, 2022. **45**(8): p. 2410-2427.
18. Steed, G., et al., *Chronoculture, harnessing the circadian clock to improve crop yield and sustainability.* Science, 2021. **372**(6541): p. eabc9141.
19. Belbin, F.E., et al., *Integration of light and circadian signals that regulate chloroplast transcription by a nuclear-encoded sigma factor.* New Phytologist, 2017. **213**(2): p. 727-738.
20. Noordally, Z.B., et al., *Circadian control of chloroplast transcription by a nuclear-encoded timing signal.* Science, 2013. **339**(6125): p. 1316-1319.
21. Onda, Y., et al., *Light induction of Arabidopsis SIG1 and SIG5 transcripts in mature leaves: differential roles of cryptochrome 1 and cryptochrome 2 and dual function of SIG5 in the recognition of plastid promoters.* The Plant Journal, 2008. **55**(6): p. 968-978.
22. Nagashima, A., et al., *The multiple-stress responsive plastid sigma factor, SIG5, directs activation of the psbD blue light responsive promoter (BLRP) in Arabidopsis thaliana.* Plant and Cell Physiology, 2004. **45**(4): p. 357-368.
23. Yamburenko, M.V., Y.O. Zubo, and T. Börner, *Abscisic acid affects transcription of chloroplast genes via protein phosphatase 2C-dependent activation of nuclear genes: repression by guanosine-3'-5'-bisdiphosphate and activation by sigma factor 5.* The Plant Journal, 2015. **82**(6): p. 1030-1041.
24. Zhao, P., et al., *ATHB17 enhances stress tolerance by coordinating photosynthesis associated nuclear gene and ATSIG5 expression in response to abiotic stress.* Scientific Reports, 2017. **7**(1): p. article 45492.
25. Mellenthin, M., et al., *Expression of the Arabidopsis sigma factor SIG5 is photoreceptor and photosynthesis controlled.* Plants, 2014. **3**: p. 359-391.
26. Tsunoyama, Y., et al., *Blue light specific and differential expression of a plastid σ factor, Sig5 in Arabidopsis thaliana.* FEBS Letters, 2002. **516**(1-3): p. 225-228.
27. Mochizuki, T., et al., *Two independent light signals cooperate in the activation of the plastid psbD blue light-responsive promoter in Arabidopsis.* FEBS Letters, 2004. **571**(1): p. 26-30.
28. Møller, S.G., et al., *PP7 is a positive regulator of blue light signaling in Arabidopsis.* The Plant Cell, 2003. **15**(5): p. 1111-1119.
29. Davey, M.P., et al., *The UV-B photoreceptor UVR8 promotes photosynthetic efficiency in Arabidopsis thaliana exposed to elevated levels of UV-B.* Photosynthesis Research, 2012. **114**(2): p. 121-131.
30. Brown, B.A. and G.I. Jenkins, *UV-B signaling pathways with different fluence-rate response profiles are distinguished in mature Arabidopsis leaf tissue by requirement for UVR8, HY5, and HYH.* Plant Physiology, 2008. **146**(2): p. 576-588.
31. Tsunoyama, Y., et al., *Blue light-induced transcription of plastid-encoded psbD gene is mediated by a nuclear-encoded transcription initiation factor, AtSig5.* Proceedings of the National Academy of Sciences of the United States of America, 2004. **101**(9): p. 3304-3309.
32. Shimmura, S., et al., *Comparative analysis of chloroplast psbD promoters in terrestrial plants.* Frontiers in Plant Science, 2017. **8**: p. article 1186.
33. Wenden, B., et al., *Light inputs shape the Arabidopsis circadian system.* The Plant Journal, 2011. **66**(3): p. 480-491.
34. Fraser, D.P., et al., *Phytochrome A elevates plant circadian-clock components to suppress shade avoidance in deep-canopy shade.* Proceedings of the National Academy of Sciences, 2021. **118**(27): p. e2108176118.

35. Panter, P.E., et al., *Circadian regulation of the plant transcriptome under natural conditions.* Frontiers in Genetics, 2019. **10**: p. article 1239.
36. Locke, J.C.W., A.J. Millar, and M.S. Turner, *Modelling genetic networks with noisy and varied experimental data: the circadian clock in Arabidopsis thaliana.* Journal of Theoretical Biology, 2005. **234**(3): p. 383-393.
37. Aikawa, S., et al., *Robust control of the seasonal expression of the Arabidopsis FLC gene in a fluctuating environment.* Proceedings of the National Academy of Sciences, 2010. **107**(25): p. 11632-11637.
38. Nishio, H., et al., *Repressive chromatin modification underpins the long-term expression trend of a perennial flowering gene in nature.* Nature Communications, 2020. **11**(1): p. article 2065.
39. Pittendrigh, C.S. and D. Skopik Steven, *Circadian Systems, V. The driving oscillation and the temporal sequence of development.* Proceedings of the National Academy of Sciences, 1970. **65**(3): p. 500-507.
40. Finster, S., et al., *Light-dependent, plastome-wide association of the plastid-encoded RNA polymerase with chloroplast DNA.* Plant Journal, 2013. **76**(5): p. 849-860.
41. Hoffer, P.H. and D.A. Christopher, *Structure and blue-light-responsive transcription of a chloroplast psbD promoter from Arabidopsis thaliana.* Plant Physiology, 1997. **115**(1): p. 213-222.
42. Satoh, J., et al., *Developmental stage-specific multi-subunit plastid RNA polymerases (PEP) in wheat.* Plant Journal, 1999. **18**(4): p. 407-415.
43. Baena-González, E., et al., *Chloroplast transcription at different light intensities. Glutathione-mediated phosphorylation of the major RNA polymerase involved in redox-regulated organellar gene expression.* Plant Physiology, 2001. **127**(3): p. 1044-1052.
44. Nakamura, T., et al., *Array-based analysis on tobacco plastid transcripts: Preparation of a genomic microarray containing all genes and all intergenic regions.* Plant and Cell Physiology, 2003. **44**(8): p. 861-867.
45. Bieniawska, Z., et al., *Disruption of the Arabidopsis circadian clock is responsible for extensive variation in the cold-responsive transcriptome.* Plant Physiology, 2008. **147**(1): p. 263-279.
46. Gould, P.D., et al., *The molecular basis of temperature compensation in the Arabidopsis circadian clock.* The Plant Cell, 2006. **18**(5): p. 1177-1187.
47. Gould, P.D., et al., *Network balance via CRY signalling controls the Arabidopsis circadian clock over ambient temperatures.* Molecular Systems Biology, 2013. **9**(1): p. article 650.
48. Mizuno, T., et al., *Ambient temperature signal feeds into the circadian clock transcriptional circuitry through the EC night-time repressor in Arabidopsis thaliana.* Plant and Cell Physiology, 2014. **55**(5): p. 958-976.
49. Thines, B. and G. Harmon Frank, *Ambient temperature response establishes ELF3 as a required component of the core Arabidopsis circadian clock.* Proceedings of the National Academy of Sciences, 2010. **107**(7): p. 3257-3262.
50. Catalá, R., J. Medina, and J. Salinas, *Integration of low temperature and light signaling during cold acclimation response in Arabidopsis.* Proceedings of the National Academy of Sciences, 2011. **108**(39): p. 16475-16480.
51. Burko, Y., et al., *Chimeric activators and repressors define HY5 activity and reveal a light-regulated feedback mechanism.* The Plant Cell, 2020. **32**(4): p. 967-983.
52. Shimizu, M., et al., *Sigma factor phosphorylation in the photosynthetic control of photosystem stoichiometry.* Proceedings of the National Academy of Sciences, 2010. **107**(23): p. 10760-10764.
53. Ling, Q. and P. Jarvis, *Regulation of chloroplast protein import by the ubiquitin E3 ligase SP1 is important for stress tolerance in plants.* Current Biology, 2015. **25**(19): p. 2527-2534.

54. Michael, T.P., P.A. Salomé, and C.R. McClung, *Two Arabidopsis circadian oscillators can be distinguished by differential temperature sensitivity.* Proceedings of the National Academy of Sciences, 2003. **100**(11): p. 6878-6883.
55. Kudoh, H., et al., *The long-term "in natura" study sites of Arabidopsis halleri for plant transcription and epigenetic modification analyses in natural environments*, in *Plant Transcription Factors: Methods and Protocols*, N. Yamaguchi, Editor. 2018, Springer New York: New York, NY. p. 41-57.
56. Honjo, M.N. and H. Kudoh, *Arabidopsis halleri: a perennial model system for studying population differentiation and local adaptation.* AoB PLANTS, 2019. **11**(6): p. article plz076.
57. Briskine, R.V., et al., *Genome assembly and annotation of Arabidopsis halleri, a model for heavy metal hyperaccumulation and evolutionary ecology.* Molecular Ecology Resources, 2017. **17**(5): p. 1025-1036.
58. Kawagoe, T. and H. Kudoh, *Escape from floral herbivory by early flowering in Arabidopsis halleri subsp. gemmifera.* Oecologia, 2010. **164**(3): p. 713-720.
59. Kamitani, M., et al., *RNA-Seq reveals virus–virus and virus–plant interactions in nature.* FEMS Microbiology Ecology, 2016. **92**(11): p. article fiw176.
60. Franklin, K.A., *Shade avoidance.* New Phytologist, 2008. **179**(4): p. 930-944.

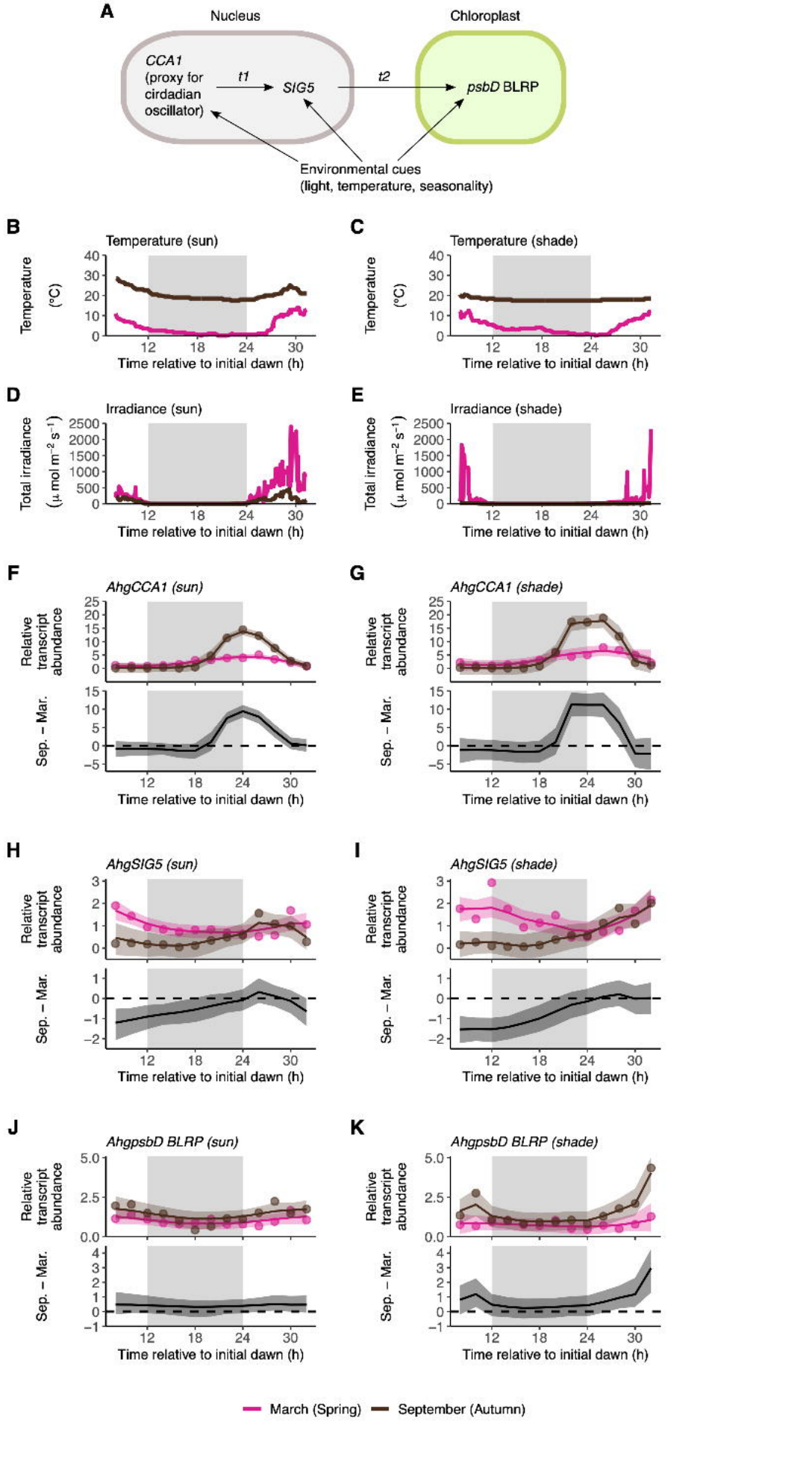
A
Nucleus
Chloroplast
CCA1
(proxy for
cirdadian
oscillator)
t1
SIG5
t2
psbD BLRP
Environmental cues
(light, temperature, seasonality)
B
Temperature (sun)
Temperature (°C)
Time relative to initial dawn (h)
C
Temperature (shade)
D
Irradiance (sun)
Total irradiance (µ mol m⁻² s⁻¹)
E
Irradiance (shade)
F
AhgCCA1 (sun)
Relative transcript abundance
Sep. – Mar.
G
AhgCCA1 (shade)
H
AhgSIG5 (sun)
I
AhgSIG5 (shade)
J
AhgpsbD BLRP (sun)
K
AhgpsbD BLRP (shade)
March (Spring)
September (Autumn)

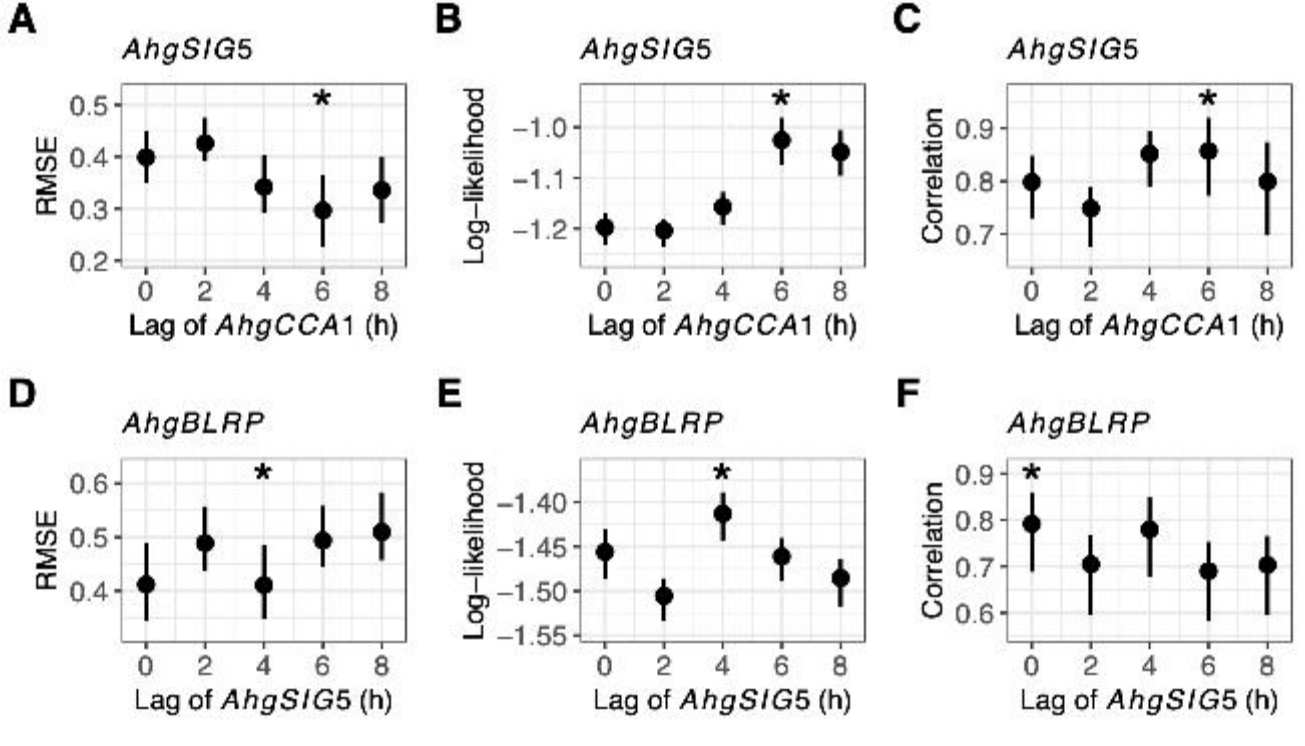
A
AhgSIG5
RMSE
0.5
0.4
0.3
0.2
*
0
2
4
6
8
Lag of AhgCCA1 (h)
B
AhgSIG5
Log−likelihood
−1.0
−1.1
−1.2
*
0
2
4
6
8
Lag of AhgCCA1 (h)
C
AhgSIG5
Correlation
0.9
0.8
0.7
*
0
2
4
6
8
Lag of AhgCCA1 (h)
D
AhgBLRP
RMSE
0.6
0.5
0.4
*
0
2
4
6
8
Lag of AhgSIG5 (h)
E
AhgBLRP
Log−likelihood
−1.40
−1.45
−1.50
−1.55
*
0
2
4
6
8
Lag of AhgSIG5 (h)
F
AhgBLRP
Correlation
0.9
0.8
0.7
0.6
*
0
2
4
6
8
Lag of AhgSIG5 (h)

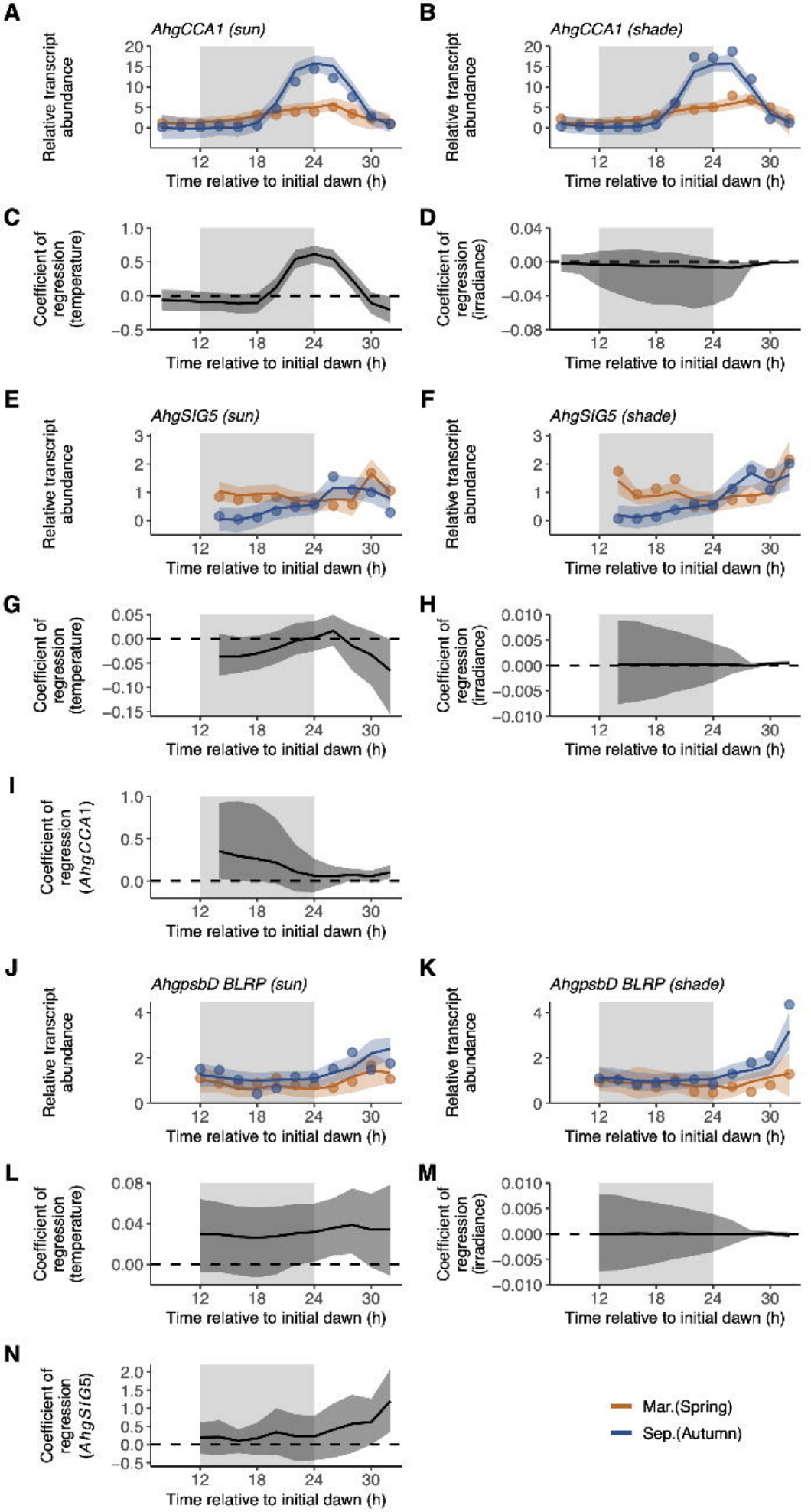
A
AhgCCA1 (sun)
Relative transcript abundance
Time relative to initial dawn (h)
B
AhgCCA1 (shade)
C
Coefficient of regression (temperature)
D
Coefficient of regression (irradiance)
E
AhgSIG5 (sun)
F
AhgSIG5 (shade)
G
H
I
Coefficient of regression (AhgCCA1)
J
AhgpsbD BLRP (sun)
K
AhgpsbD BLRP (shade)
L
M
N
Coefficient of regression (AhgSIG5)
Mar.(Spring)
Sep.(Autumn)

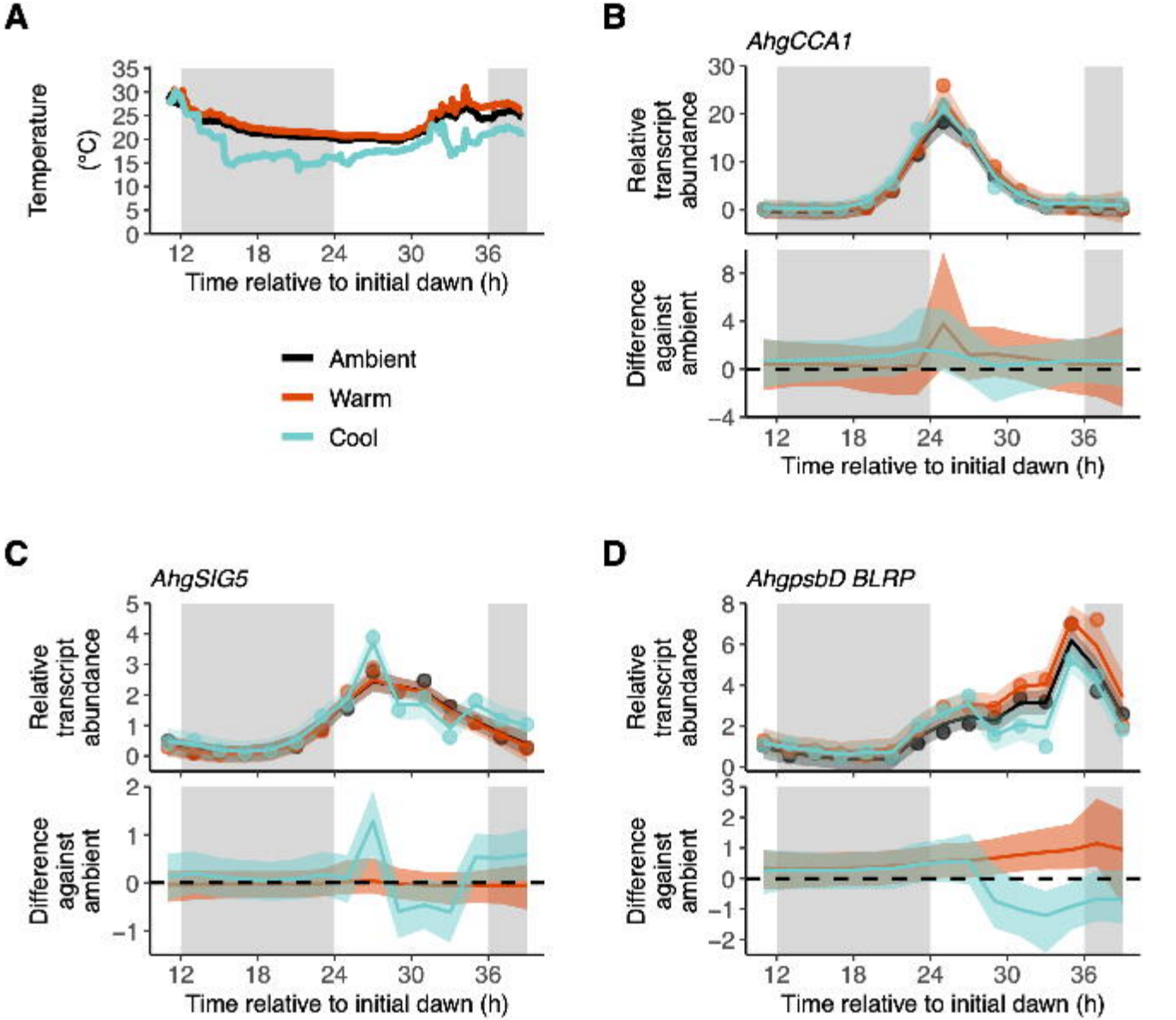
A
Temperature (°C)
35
30
25
20
15
10
5
0
12
18
24
30
36
Time relative to initial dawn (h)
Ambient
Warm
Cool
B
AhgCCA1
Relative transcript abundance
30
20
10
0
Difference against ambient
8
4
0
−4
12
18
24
30
36
Time relative to initial dawn (h)
C
AhgSIG5
Relative transcript abundance
5
4
3
2
1
0
Difference against ambient
2
1
0
−1
12
18
24
30
36
Time relative to initial dawn (h)
D
AhgpsbD BLRP
Relative transcript abundance
8
6
4
2
0
Difference against ambient
3
2
1
0
−1
−2
12
18
24
30
36
Time relative to initial dawn (h)